Response of the Electric Field Gradient in Ion implanted $BaTiO_3$ to an External Electric Field

Marc Dietrich, Jörn Bartels[1], Manfred Deicher, Kristian Freitag[1], Vyacheslav Samokhvalov[2] and Sepp Unterricker[2]
Fachbereich Physik, Universität Konstanz, D-78457 Konstanz, Germany
[1]Institut für Strahlen- und Kernphysik, Universität Bonn, D-53115 Bonn, Germany
[2]Institut für Angewandte Physik, TU Bergakademie Freiberg, D-09596 Freiberg, Germany

ABSTRACT

Single crystalline, ferroelectric $BaTiO_3$ as material with the highest piezoelectric constants among the perovskites with ordered sublattices was implanted with $^{111}In(^{111}Cd)$. The electric field gradient at the Ti position was measured with perturbed $\gamma\gamma$-angular correlation spectroscopy (PAC) while the crystal was exposed to an external electric field. A quadratic dependence could be observed: $\nu_Q(E) = (34.8(1) + 0.16(4)\ E/kV/mm + 0.080(2)\ E^2/kV^2/mm^2)$ MHz. Point charge model calculations reproduce the linear change of V_{zz}, but not the quadratic term. The polarizability of the host ions of $BaTiO_3$ is known to be nonlinear with respect to an electric field. The resulting quadratic shift of the electron density is reflected in the strength of the EFG.

INTRODUCTION

In solids, the electric field gradient (EFG) at a certain lattice site is determined mainly by the atoms in its nearest neighborhood, i.e. their electronic properties and the distances to each other. Therefore, variations of lattice constants lead to changes in EFG. Lattice constants change when the temperature is varied. Such studies have been performed for numerous materials with perturbed $\gamma\gamma$-angular correlation spectroscopy (PAC) [1]. A few papers report on the response of the EFG on hydrostatic pressure [2] or on the bending angle of a single crystal [3].

Another way of applying uniaxial stress can be achieved by the inverse piezoelectric effect. In polar crystals lattice constants change or atoms are shifted when an electric field is applied externally resulting in an influence on the EFG at lattice sites. We have carried out experiments in order to observe these slight changes in $LiNbO_3$ with PAC recently. The measurements revealed only a tiny change of the EFG in dependence on the external electric field.

In this report we present further studies using a different material. The primary requirement for the success of such an experiment is a high piezoelectric constant of the material. Solids used as piezoelectric actuators with very high piezoelectric constants like $Sr_xBa_{1-x}NbO_3$ are not useful for PAC investigations because of the random occupation of the Ba sublattice by Ba and Sr atoms. This would result in a strongly damped spectrum since the probes are not exposed to an unique EFG. Therefore we have chosen $BaTiO_3$ as an ordered material with piezoelectric constants larger than those of $LiNbO_3$.

Calculations of EFG at lattice sites in $BaTiO_3$ with WIEN97 [4] using the FP-LAPW method will be presented. Since these first principles calculations are rather complex, we have chosen a

much more easy way of naive point charge model calculations [5] in order to simulate the behaviour of EFG under uniaxial strain.

EXPERIMENTAL DETAILS

$BaTiO_3$ crystallizes in the Perovskite structure and exhibits at room temperature a tetragonal ferroelectric phase. The single crystalline sample from 'Forschungsinstitut für mineralische und metallische Werkstoffe - Edelsteine/Edelmetalle - GmbH', Idar-Oberstein, had a size of 6 x 8 mm^2 and a thickness of 1 mm. The polar axis along c was perpendicular to the plane. The sample had been prepared from a crystal grown with 100 ppm Co in the melt for optoelectronics use. $BaTiO_3$ is very attractive as material for optical and holographic storage [6] and optical waveguides [7]. PAC studies in this material have been carried out with different nuclear probes for almost three decades, already [8-10].

We have implanted ^{111}In(^{111}Cd) at the isotope separator at Bonn university with an energy of 160 keV and a dose of 2.2×10^{13} cm^{-2} and a beam spot of 5 mm diameter. In order to remove the implantation damage the sample has been annealed for 2.5 h at 1700 K in air. The crystal was adjusted in a special Teflon holder to apply the electric field. The c-axis and consequently the symmetry axis of the EFG were oriented perpendicular to the detector plane. Aluminum electrodes with a diameter of 6 mm covered the implanted area. Transformer oil with a breakdown field strength of 6 kV/mm has been used for insulation. The breakdown field strength of the sample is much higher, about 40 kV/mm for nominally undoped $BaTiO_3$ [11].

The PAC technique [12] is sensitive to electric field gradients (EFG) present at the site of the probe atom ^{111}In(^{111}Cd). The EFG reflects the deviation the electron charge density from cubic symmetry. An EFG causes a hyperfine splitting of an excited state of the ^{111}Cd nuclei. The EFG is mainly described by the quadrupole coupling constant

$$\nu_Q = eQV_{zz}/h \quad (1)$$

(Q - nuclear quadrupole moment, V_{zz} - largest component of diagonalized EFG tensor). This quantity is measured by PAC and unique for a lattice site in defect free material. The fraction of probe atoms involved in this complex can be determined from the characteristic modulation of the PAC spectrum R(t). A small damping of the observed modulation due to the superposition of slightly different EFG caused by defects relatively far away from the probe atom is described by the width $\Delta\nu_Q$ assuming a Lorentzian distribution of these EFG. The PAC-measurements have been carried out at ambient temperature.

Calculations of EFG were performed with the WIEN97 implementation [4] of the Full-Potential Linearized-Augmented-Plane-Wave (FP-LAPW) method [13]. We worked in the GGA (generalized gradient approximation), in which recent progress has been made going beyond the LSDA (the local spin density approximation) by adding gradient terms of the electron density to the exchange-correlation energy or its corresponding potential [14]. For methodological purposes the unit cell is divided into non-overlapping spheres with radius R_{MT} (muffin-tin radius) and an interstitial region. The atomic spheres radii for $BaTiO_3$ were used as follows: R_{MT}(Ba) = 2.3 Å, R_{MT}(Ti) = 1.7 Å, R_{MT}(O1) = 1.8 Å and R_{MT}(O2) = 2.0 Å, respectively. We took for the parameter R_{Kmax}, which controls the size of the basis-set in these calculations, the value of 8.

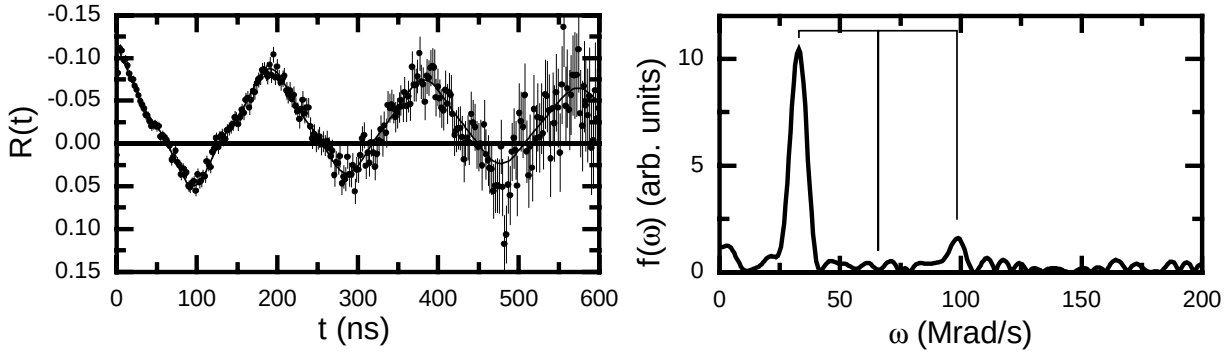

Figure 1. *PAC spectrum and its Fourier transform of $^{111}In(^{111}Cd)$ implanted into a $BaTiO_3$ single crystal. The sample has been annealed at 1700 K for 2.5 h. The c-axis has been oriented perpendicular to the detector plane.*

Integration in reciprocal space was performed using the tetrahedron method taking 500 k-points in the whole Brillouin zone. As convergence parameter the charge convergence criterion of 0.0005 was chosen. The value of 14 for G_{MAX} (the magnitude of the largest vector in charge density Fourier expansion) was used. The lattice parameters were taken from [15]: a = b = 3.9945 Å, c = 4.0335 Å, z(Ti) = 0.5153, z(O1) = -0.024, z(O2) = 0.4850.

Point charge model calculations have been carried out starting with same atomic positions [15]. The lattice contributions to the EFG at the Ti-site have been calculated. The deformation of the unit cell caused by the external electric field has been taken into account as changes in the lattice constants. The electric field along the c-axis causes a strain along both the c- and the a-axis. The relative changes for a field of 4 kV/mm are $\Delta a/a = 1.6\times10^{-4}$ and $\Delta c/c = -1.4\times10^{-4}$. The signs depend on the direction of the electric field with respect to the direction of the spontaneous polarization and are opposite to each other in any case.

RESULTS

The PAC spectrum and its Fourier transform of $^{111}In(^{111}Cd)$ in $BaTiO_3$ are shown in figure 1. 90(5) % of the probes are exposed to an axially symmetric EFG with the quadrupole coupling constant of ν_Q = 34.8(1) MHz and a distribution of $\Delta\nu_Q$ = 1.0(1) MHz. The second harmonic is not visible in the Fourier transform due to the special orientation of the crystal. A number of arguments indicate the substitution of $^{111}In(^{111}Cd)$ on the Ti-site [8]. One of these is the comparison of the measured EFG with those measured by NMR, which is host element specific, and with results of calculations. For this purpose, the largest component V_{zz} of the EFG at the Ba- and Ti-site in $BaTiO_3$ are summarized in table 1. With $^{111}In(^{111}Cd)$ a single EFG has been measured. The values for V_{zz} at the Ba- and Ti-sites have been calculated from the measured value of the EFG at the position of $^{111}In(^{111}Cd)$ according to

$$V_{zz,Ti} = (1-\gamma_\infty)_{Ti}/(1-\gamma_\infty)_{Cd}\, V_{zz,Cd} \quad (2)$$

($V_{zz,X}$ = largest component of EFG observed with atom X at a certain lattice site, $(1-\gamma_\infty)_X$ = Sternheimer factor for an ion of element X [16]). The value for $^{111}In(^{111}Cd)$ at the Ba-site is one

	lattice site	PAC $^{111}In(^{111}Cd)$	NMR [17]	Theory	Theory [18]	
				T = 0 K	T = 0 K	T = 296 K
V_{zz} in 10^{20} V/m^2	Ba	(54.5(2))	4.35	5.6	2.97	6.00
	Ti	5.72(2)	6.82	3.1	0.59	6.85
	O1			8.9		
	O2			12.8		

Table 1. *Largest component V_{zz} of the electric field gradient at the Ba- and Ti-site in $BaTiO_3$. With $^{111}In(^{111}Cd)$ a single EFG has been measured which is expected to be the one at the Ti-site [8]. Nevertheless, the value that $^{111}In(^{111}Cd)$ at the Ba-site would give is written in brackets. More NMR results with ^{47}Ti, ^{49}Ti and ^{137}Ba have been compiled in [17]. Our theoretical approach with WIEN did not take into account lattice vibrations which is indicated as T = 0 K. The values taken from [18] have been calculated both without lattice vibrations and taking into account lattice vibrations (T = 296 K).*

order of magnitude higher than the results of both NMR and theories. Our theoretical approach with WIEN97 results in values that differ for the Ti-site by a factor of two and for the Ba-site by 30 % from the NMR-values.

The first harmonics in the Fourier spectra of measurements with electric field applied to the sample are drawn enlarged in figure 2. The electric field strength is defined as positive by connecting the non-implanted side of the crystal to the positive output of the high voltage supply. A shift of the peak to higher frequencies with increasing electric field strength is clearly visible. The corresponding quadrupole coupling constants in dependence on the electric field strength applied are shown in figure 3 for all PAC spectra recorded.
The fit to the experimental values results in the function

$$\nu_Q(E) = 34.8(1)\text{MHz} + 0.16(4)\frac{\text{MHz}}{\text{kV/mm}}\text{E} + 0.080(2)\frac{\text{MHz}}{(\text{kV/mm})^2}\text{E}^2 \quad (3).$$

DISCUSSION

The comparison of experimental and theoretical EFG in table 1 proves the substitution of $^{111}In(^{111}Cd)$ at the Ti-site as suggested in the literature [8]. Our theoretical approach with WIEN97 results in values that differ for the Ti-site by a factor of two and for the Ba-site by 30 % from the NMR-values. This may have two reasons. First, the EFG probably depends strong on the exact positions of the Ti- and O-ions in the unit cell. The calculated values may differ when using another set of atomic positions. Second, LMTO-calculations suggest a significant contribution of thermal fluctuation to the EFG [18]. WIEN97 does not take into account such lattice vibrations. Nevertheless, this contribution does not seem to be as strong as discussed in [18] since our values of the EFG differ less from the experimental ones than those calculated by LMTO without thermal fluctuations.

The linear change of the quadrupole coupling constant for $BaTiO_3$ is $\Delta\nu_Q/\Delta E = 0.16$ MHz/kV/mm. This is 10 times the value of 0.017 MHz/kV/mm observed for $LiNbO_3$. This has

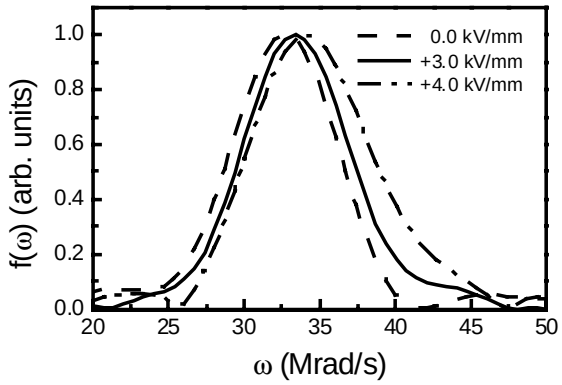

Figure 2. *Normalized Fourier transforms of PAC spectra recorded with $^{111}In(^{111}Cd)$ in $BaTiO_3$ for different externally applied electric field of 0.0 kV/mm, +3.0 kV/mm and +4.0 kV/mm indicated by the dashed, solid and dash dotted line, respectively.*

been expected looking into the piezoelectric constants. The piezoelectric strain constant d_{33} determines the strain in c-direction $S_{33} = d_{33}E_{33}$ of a Perovskite structure crystal with respect to the external electric field strength E_3 along c-axis. The strain constants are $d_{33} = 3.6\times10^{-11}$ C/N and 0.6×10^{-11} C/N for $BaTiO_3$ [19] and $LiNbO_3$ [20], respectively, and differ by a factor of 6.

The relative changes $\Delta\nu_Q/\nu_Q$ caused by the electric field strength of 1 kV/mm differ even more, by a factor of 40. The values are $\Delta\nu_Q/\nu_Q = 4.6\times10^{-3}$ ($BaTiO_3$) and 0.11×10^{-3} ($LiNbO_3$).

It turns out that the linear contribution can be simulated with point charge model calculations. The point charge model calculations result in a purely linear dependence of the EFG on the electric field strength. An electric field of 1 kV/mm causes a relative change of the quadrupole coupling constant of $\Delta\nu_Q/\nu_Q = 1\times10^{-2}$, twice the experimental value but the agreement is satisfactorily good.

The model does not propose a second order dependence. This may have two reasons. The first order effect of an external electric field is well studied concerning the influence on lattice constants. But only little information is available concerning the influence of an external electric

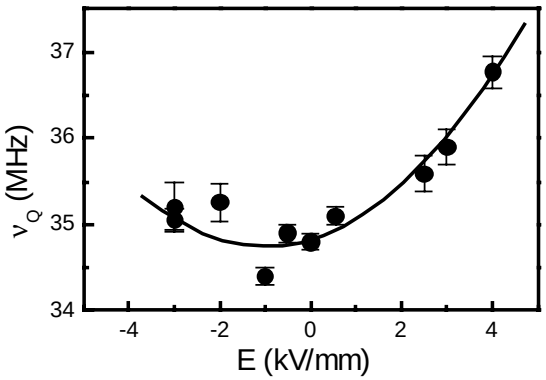

Figure 3. *Dependence of the quadrupole coupling constant ν_Q of $^{111}In(^{111}Cd)$ in $BaTiO_3$ on the externally applied electric field E. The solid line represents a fit of a second order polynomial to the values measured*

field on the atomic positions in the unit cell. One can imagine that the atoms are shifted relative to each other when a field is applied.

The polarizability of the host ions of $BaTiO_3$ is known to result in a quadratic shift of electron density with respect to an electric field strength carried by photons. When a static electric field is applied externally, the polarization occurs in a similar nonlinear way. The resulting quadratic shift of the electron density is reflected in the strength of the EFG.

CONCLUSIONS

We have shown the nonlinear dependence of the electric field gradient (EFG) at the Ti-site in $BaTiO_3$ on the strength of an external electric field. This effect is meant to reflect the nonlinear polarization of the electron shells. So, PAC spectrocsopy is feasible to be used for the investigation of the polarizability of electron shells in solids.

ACKNOWLEDGEMENT

We gratefully acknowledge the financial support of the Bundesministerium für Bildung und Forschung (03-DE5KO1-6, 03-DE5KO2-9).

REFERENCES

1. G.L. Catchen, W.E. Evenson and D. Alred, Phys. Rev., **B54**, R3679 (1996).
2. H.H. Rinneberg, G.P. Schwartz and D.A. Shirley, Hyp. Int., **3**, 97 (1977).
3. G. Marx and R. Vianden, Physics Letters, **A210**, 364 (1996).
4. P. Blaha, K. Schwarz and J. Luitz, WIEN97, (Techn. Univ. Wien 1999).
5. F.W. de Wette, Phys. Rev., **123**, 103 (1961).
6. E. Kratzig, F. Welz, R. Orlowski, V. Doormann and M. Rosenkranz, Solid State Comm., **34**, 817 (1980).
7. P. Moretti, P. Thevenard, G. Godefroy, R. Sommerfeld, P. Hertel and E.Krätzig, phys. stat. sol., **a117,** K85 (1990).
8. M. Uhrmacher, V.V. Krishnamurty, K.-P. Lieb, A. López-Garcia and M. Neubauer, Z. Phys. Chem., **206**, 249 (1998).
9. G.L. Catchen and R.L. Rasera, Ferroelectrics (UK), **120,** 33 (1991).
10. G. Schäfer, P. Herzog and B. Wolbeck, Z. Physik, **A257,** 336 (1972).
11. Landolt-Börnstein III/3, (Springer 1969).
12. G. Schatz, A. Weidinger, Nuclear condensed matter physics: nuclear methods and applications, transl. J.A. Gardner, (John Wiley & Sons, 1995).
13. E. Wimmer, H. Krakauer, M. Weinert and A.J. Freeman, Phys. Rev., **B24**, 864 (1981).
14. J.P. Perdew, S. Burke and M. Ernzerhof, Phys. Rev. Let., **77**, 3865 (1996).
15. H.D. Megaw, Acta Cryst., **15,** 972 (1962).
16. F.D. Feiock, W.R. Johnson, Phys. Rev., **187**, 39 (1969).
17. O. Kanert, H. Schulz, J. Albers, Solid State Comm., **91**, 465 (1994).
18. K.H. Weyrich, R.P. Madenach, Ferroelectrics, **111**, 9 (1990).
19. Landolt-Börnstein III/28a, (Springer, 1990).
20. Landolt-Börnstein III/16a, (Springer, 1981).